DOCTORAL THESIS

A Low Tumor Mutational Burden and *PTEN* Mutations Are Predictors of a Negative Response to PD-1 Blockade in Microsatellite instability-High (MSI-H)/deficient mismatch repair (dMMR) Gastrointestinal Tumors

(MSI-H/dMMR 消化器腫瘍において、腫瘍変異負荷低値と

PTEN 変異が抗 PD-1 抗体に対する負の予測因子となる)

March, 2022

(2022 年 3 月)

Keigo Chida

千田　圭悟

Department of Gastroenterological Surgery

Yokohama City University Graduate School of Medicine,

横浜市立大学 大学院医学研究科 医科学専攻 消化器・腫瘍外科学

(Research Supervisor: Takayuki Yoshino, Professor)

国立がん研究センター東病院　消化管内科

(研究指導教員：吉野 孝之 科長)

(Doctoral Supervisor: Itaru Endo, Professor)

(指導教員:遠藤 格 教授)

Published OnlineFirst April 29, 2021; DOI: 10.1158/1078-0432.CCR-21-0401

A Low Tumor Mutational Burden and *PTEN* Mutations Are Predictors of a Negative Response to PD-1 Blockade in MSI-H/dMMR Gastrointestinal Tumors

Keigo Chida[1,2], Akihito Kawazoe[1], Masahito Kawazu[3], Toshihiro Suzuki[4,5], Yoshiaki Nakamura[1], Tetsuya Nakatsura[4], Takeshi Kuwata[6], Toshihide Ueno[3], Yasutoshi Kuboki[1], Daisuke Kotani[1], Takashi Kojima[1], Hiroya Taniguchi[1], Hiroyuki Mano[3], Masafumi Ikeda[1], Kohei Shitara[1], Itaru Endo[2], and Takayuki Yoshino[1]

ABSTRACT

Purpose: This study performed a comprehensive molecular characterization of microsatellite instability–high (MSI-H)/mismatch repair–deficient (dMMR) gastrointestinal (GI) tumors to elucidate predictors of response to PD-1 blockade.

Experimental Design: Forty-five patients with MSI-H/dMMR GI tumors, including gastric cancer, colorectal cancer, cholangiocarcinoma, small intestine cancer, pancreatic cancer, and duodenal cancer, receiving PD-1 blockade were analyzed. We conducted the genomic profiling of GI tumors by whole-exome sequencing or targeted next-generation sequencing. The tumor microenvironment was evaluated by transcriptomic analysis and multiplex fluorescence IHC.

Results: Patients with low tumor mutational burdens (TMBs) had lower objective response rates (ORRs; 0% vs. 48.8%) and a significantly shorter progression-free survival (PFS; 2.3 vs. 15.6 months; HR, 6.20; $P = 0.002$) than those with high TMBs. Among common gene alterations in GI tumors, only *PTEN* mutations, which were mutually exclusive with a low TMB, were significantly associated with a lower ORRs than wild-type *PTEN* (21.4 vs. 54.8%; odds, 4.45; $P = 0.045$). Compared with wild-type *PTEN, PTEN* mutations in the phosphatase domain were associated with significantly lower ORRs (12.5 vs. 54.8%; $P = 0.049$), shorter PFS (2.6 vs. 15.6 months; HR, 5.04; $P < 0.001$), lower intratumoral $CD8^+$ T-cell levels, higher intratumoral $CD204^+$ macrophage levels, and PI3K/AKT/mTOR pathway enrichment, whereas *PTEN* mutations in the C2 domain were not.

Conclusions: Low TMBs and *PTEN* mutations, especially mutations in the phosphatase domain associated with an immunosuppressive environment, were mutually exclusive and might be negative predictors of PD-1 blockade responses in patients with MSI-H/dMMR GI tumors.

Introduction

Microsatellite instability–high (MSI-H) or mismatch repair–deficient (dMMR) tumors exhibit frequent mutations in multiple genes, contributing to the enhanced expression of neoantigens, increased $CD8^+$ T-cell infiltration, and expression of related immune checkpoint molecules in the tumor microenvironment (1, 2). Immune checkpoint inhibitors, such as PD-1 blockade, have shown improved survival outcomes in patients with MSI-H or dMMR gastrointestinal (GI) tumors, including hepatobiliary and pancreatic cancers (3, 4). In the KEYNOTE-177 phase III study, pembrolizumab demonstrated better clinical outcomes than standard chemotherapy for patients with MSI-H/dMMR colorectal cancer in a first-line setting (5). Exploratory analysis from phase II and III studies of pembrolizumab for gastric cancer showed remarkable benefits of pembrolizumab compared with chemotherapy (6, 7). However, approximately half of the patients in these pivotal trials showed early disease progression, highlighting the importance of identifying predictive biomarkers associated with unresponsiveness to PD-1 blockade.

To date, PD-L1 expression and several gene alterations have been reported to be associated with the efficacy of immune checkpoint inhibitors in microsatellite-stable (MSS)/MMR-proficient (pMMR) solid tumors (8–11). In addition, tumor mutational burden (TMB), a potential indicator of tumor immunogenicity, has been reported to be associated with the efficacy of PD-1 blockade independent of MSI status (3, 12). In contrast, predictive biomarkers of the efficacy of immune checkpoint inhibitors for MSI-H/dMMR GI tumors are not well established (12). Thus, uncovering molecular determinants of the response to immune checkpoint inhibitors might aid in the development of novel biomarkers or combination therapies to overcome resistance to these agents in MSI-H/dMMR tumors.

Here, to elucidate predictors of response to immune checkpoint inhibitors in MSI-H/dMMR GI tumors, we explored the comprehensive molecular landscape through whole-exome sequencing (WES) or targeted next-generation sequencing (NGS), transcriptomic analysis, and multiplex fluorescence IHC in patients with MSI-H/dMMR GI tumors receiving PD-1 blockade.

[1]National Cancer Center Hospital East, Kashiwa, Chiba, Japan. [2]Department of Gastroenterological Surgery, Yokohama City University Graduate School of Medicine, Yokohama, Japan. [3]Division of Cellular Signaling, National Cancer Center Research Institute, Tokyo, Japan. [4]Division of Cancer Immunotherapy, Exploratory Oncology Research and Clinical Trial Center, National Cancer Center, Kashiwa, Japan. [5]General Medicinal Education and Research Center, Teikyo University, Tokyo, Japan. [6]Department of Pathology and Clinical Laboratories, National Cancer Center Hospital East, Kashiwa, Japan.

Note: Supplementary data for this article are available at Clinical Cancer Research Online (http://clincancerres.aacrjournals.org/).

K. Chida and M. Kawazu contributed equally to this article.

Corresponding Author: Akihito Kawazoe, Department of Gastroenterology and Gastrointestinal Oncology, National Cancer Center Hospital East, 6-5-1 Kashiwanoha, Kashiwa, Chiba 277-8577, Japan. Phone: 81-47-133-1111; Fax: 81-47-134-6928; E-mail: akawazoe@east.ncc.go.jp

Clin Cancer Res 2021;27:3714–24

doi: 10.1158/1078-0432.CCR-21-0401

Published OnlineFirst April 29, 2021; DOI: 10.1158/1078-0432.CCR-21-0401

Translational Relevance

Approximately half of microsatellite instability–high (MSI-H)/mismatch repair–deficient (dMMR) tumors do not respond to PD-1 blockade, indicating the importance of the identification of predictive biomarkers associated with less responsiveness to PD-1 blockade. Among 45 MSI-H/dMMR gastrointestinal tumors, a low tumor mutational burden (TMB) and *PTEN* mutations were mutually exclusive and were associated with poor clinical outcomes to PD-1 blockade. *PTEN* mutations in the phosphatase domain were associated with lower responsiveness to PD-1 blockade together with decreased $CD8^+$ T cells and increased tumor-associated macrophages, whereas those in the C2 domain were not. Importantly, among 20 patients showing disease progression within 6 months after PD-1 blockade, four had a low TMB (20%) and eight had *PTEN* phosphatase domain mutations (40%). Other gene alterations, such as *STK11, FBXW7, JAK1, B2M,* and *HLA mutations*, were also observed in nonresponders.

Materials and Methods

Patients

We performed a comprehensive molecular analysis to evaluate associations of molecular features with the efficacy of PD-1 blockade in patients with MSI-H or dMMR advanced GI tumors at our institution. The inclusion criteria were as follows: (i) an Eastern Cooperative Oncology Group performance status of 0 to 1; (ii) histologically proven, unresectable, locally advanced, or metastatic GI tumor (refractory or intolerant to one or more chemotherapies; (iii) MSI-H or dMMR status verified by local PCR or IHC testing (described below); (iv) adequate bone marrow, hepatic, and renal function as indicated by medical records; and (v) received an anti–PD-1 inhibitor alone (pembrolizumab or nivolumab) or as combination therapy (pembrolizumab plus napabucasin; ref. 13) from July 2015 to June 2020. All patients provided written informed consent for the biomarker analysis of formalin-fixed paraffin-embedded (FFPE) tissue specimens from archival tissue samples. The study protocol was approved by the Institutional Review Board of the National Cancer Center Hospital East (Kashiwa, Chiba, Japan), and this study was conducted in accordance with the guidelines for biomedical research specified in the Declaration of Helsinki.

MSI and MMR status

MSI status was analyzed using a Promega MSI analysis system (five mononucleotide markers for the detection of MSI: BAT-25, BAT-26, NR-21, NR-24, and MONO-27; Promega; ref. 14), and tumors were classified as MSI-H if instability was noted in a minimum of two markers. MMR status was assessed by IHC using the following mAbs: anti-mutL homolog 1 (MLH1, ES05), anti-mutS homolog 2 (MSH2, FE11), antipostmeiotic segregation increased 2 (PMS2, EP51), and anti-mutS homolog 6 (MSH6, EP49; Agilent Technologies). Tumors that lacked either MLH1, MSH2, PMS2, or MSH6 expression were considered dMMR.

Genomic analysis

For WES, genomic DNA was isolated from FFPE specimens using a GeneRead DNA FFPE kit (QIAGEN), and exonic fragments were enriched using a Human Core Exome kit with RefSeq spike-in (both from Twist Bioscience). Massively parallel sequencing of prepared libraries was performed on a NovaSeq 6000 system (Illumina). Copy-number status was analyzed using our in-house pipeline, and details are provided in the Supplementary Methods. Amplification was defined as a copy number of five or more. The details of WES analysis are available in the Supplementary Methods. If patients underwent NGS-targeted gene panel analysis [Oncomine Cancer Research Panel (Thermo Fisher Scientific), FoundationOne Liquid (Foundation Medicine), or Guardant 360 (Guardant Health)] before this study, these genomic data were also collected. Genomic characterization was analyzed by focusing on the common oncogenic signaling pathways (15). TMB was defined as the total number of nonsynonymous mutations, including indels, mutations per megabase (muts/Mb) in WES, the Oncomine Cancer Research Panel, or FoundationOne Liquid. TMB-high was defined as ≥10 muts/Mb using these assays. In Guardant 360, TMB was determined by normalizing to the mutational burden expected for the tumor type and ctDNA fraction, as derived from a training set of 10,543 consecutive clinical samples, and is reported as the TMB score (16). Among these samples, the top 2% were defined as TMB-high.

Total RNA was extracted from FFPE specimens with an RNeasy FFPE kit (QIAGEN). Ribosomal RNA was depleted from total RNA with an NEBNext rRNA Depletion kit (New England Biolabs). Sequencing libraries for RNA sequencing (RNA-seq) were prepared with an NEBNext Ultra RNA Library Prep kit (New England Biolabs). Prepared RNA-seq libraries underwent 150-bp, paired-end NGS sequencing. Enriched pathways were determined using the gene set enrichment analysis (GSEA) tool available from the Broad Institute website (https://www.gsea-msigdb.org/gsea/index.jsp). Hallmark gene sets were downloaded from the Molecular Signatures Database (17).

Multiplex immunofluorescence IHC and PD-L1 expression

The protein expression levels of CD3, CD4, CD8, CD204, cytokeratin, and PTEN in FFPE samples were assessed using multiplex fluorescence IHC with each mAb. The details of multiplex immunofluorescence are available in the Supplementary Methods.

The PD-L1 combined positive score (CPS) was assessed by a trained pathologist (T. Kuwata) who was blinded to the diagnoses and/or other identifying information using PD-L1 IHC 22C3 pharmDx (Dako) and was defined as the ratio of the number of PD-L1–positive cells (tumor cells, lymphocytes, and macrophages) to the total number of tumor cells multiplied by 100.

Outcomes and statistical analysis

The efficacy endpoints were the objective response rate (ORR), disease control rate (DCR), progression-free survival (PFS), and overall survival (OS). Tumor response was assessed in patients with measurable lesions using the RECIST version 1.1. The ORR was defined as the proportion of patients whose best overall response was a complete response (CR) or partial response (PR). The DCR was defined as the proportion of patients who achieved a best overall response of a CR, PR, or stable disease (SD) lasting more than 6 weeks from the start of study treatment. PFS was defined as the time from study treatment initiation to disease progression or death from any cause. OS was defined as the time from study treatment initiation to death from any cause.

Quantitative data are expressed as the median and interquartile range (IQR). The Mann–Whitney *U* test was used to compare continuous variables, and the Fisher exact test was used to compare categorical variables. The ORRs according to the mutational status and the PD-L1 CPS were calculated as the OR using the logistic regression method. The PFS and OS were estimated using the Kaplan–

Published OnlineFirst April 29, 2021; DOI: 10.1158/1078-0432.CCR-21-0401

Meier method and compared according to each molecular status associated with a low ORR by univariate and multivariate analyses using Cox proportional hazards models. The backward selection method was conducted for the selection of factors retained in the multivariate analysis ($P < 0.1$). All P values < 0.05 were considered statistically significant. All statistical analyses were performed using the statistical program R version 4.0.3 (The R Foundation for Statistical Computing). All statistical analyses were performed using the statistical program R version 4.0.3 (The R Foundation for Statistical Computing).

Results

Patient overview

To examine patient characteristics associated with response to PD-1 blockade, we identified patients with GI tumors and evaluated their characteristics and responses to PD-1 blockade. A total of 45 patients met the inclusion criteria and had the following cancers: gastric cancer ($n = 18$), colorectal cancer ($n = 17$), cholangiocarcinoma ($n = 5$), small intestine cancer ($n = 2$), pancreatic cancer ($n = 2$), and duodenal cancer ($n = 1$; **Table 1**). All tumor specimens were collected from primary tumor samples before PD-1 blockade; 23 were biopsy specimens, and 22 were surgical specimens. WES was conducted in tumor samples from 40 patients, and the results from NGS testing were also collected from 33 patients. The maximum percentage change in tumor size from baseline was shown in **Fig. 1**. All patients had measurable lesions. In the overall population, the ORR and DCR were 44.4% (20 of 45 patients) and 84.4% (38 of 45 patients), respectively. The median follow-up at the time of the analysis was 25.3 months. In the overall population, the median PFS was 9.6 months [95% confidence interval (CI), 4.2–not reached], and the median OS was 23.2 months (95% CI, 8.4–not reached), with 23 patients (51.1%) dying (Supplementary Fig. S1).

Table 1. Baseline patient characteristics.

	***N* = 45**
Age	
Median (range)	68 (30–84)
≥65, *n* (%)	24 (53.3)
Sex, *n* (%)	
Male	24 (53.3)
Female	21 (46.7)
ECOG PS, *n* (%)	
0	26 (57.8)
1	19 (42.2)
Previous treatment regimens, *n* (%)	
1	18 (40.0)
≥2	27 (60.0)
Primary cancer, *n* (%)	
Gastric	18 (40.0)
Colorectal	17 (37.8)
Cholangiocarcinoma	5 (11.1)
Small intestine	2 (4.4)
Pancreatic	2 (4.4)
Duodenal	1 (2.2)
Metastatic sites, *n* (%)	
Liver	9 (20.0)
Lung	7 (15.6)
Lymph node	35 (77.8)
Peritoneum	20 (44.4)
Number of metastatic organs, *n* (%)	
1	23 (51.1)
≥2	22 (48.9)
Treatment, *n* (%)	
Nivolumab	8 (17.8)
Pembrolizumab	29 (64.4)
Pembrolizumab with napabucasin	8 (17.8)
TMB mutations/Mb, median (range)	38.7 (3.6–93.0)

Abbreviations: ECOG, Eastern Cooperative Oncology Group; PS, Performance status.

Among patients with colorectal cancer ($n = 17$), four had $BRAF^{V600E}$ mutation, which is not usually observed in Lynch syndrome (LS) with germline mutations. Thus, these four patients were considered to be non-LS. Among the remaining 13 patients, eight undertook genetic testing. Then, five patients were diagnosed as LS with germline mutation and three were as non-LS (a total of seven were non-LS). The ORR, median PFS, and OS [LS ($n = 5$) vs. non-LS ($n = 7$)] were as follows: (ORR, 40.0% vs. 42.9%; $P = 1.000$), [median PFS, not reached (95% CI, 3.0–not reached) vs. 15.6 months (95% CI, 1.1–reached); HR, 0.66 (95% CI, 0.12–3.60), $P = 0.628$], and [median OS, 31.0 months (95% CI, 5.3–not reached) vs. 23.2 months (95% CI, 2.6–not reached); HR, 0.41 (95% CI, 0.04–3.95), $P = 0.423$].

Molecular features associated with the response to PD-1 blockade

Comprehensive molecular characterization in association with the response to PD-1 blockade is shown in **Fig. 2**. The median TMB assessed by WES was 38.7 muts/Mb ($n = 40$; range, 3.6–93.0 muts/Mb; **Table 1**). Among 45 patients, 36 patients had TMB-high tumors (≥10 muts/Mb), and the remaining four patients had TMB-low tumors (<10 muts/Mb; **Fig. 2**; Supplementary Table S1). Three of four patients with TMB-low tumors had gastric cancer, and the remaining patient had colorectal cancer (Supplementary Table S1). All patients ($n = 5$) assessed by the NGS-targeted panel had TMB-high tumors (**Fig. 2**). No patients with TMB-low tumors showed an objective response (CR or PR) to PD-1 blockade (**Table 2**). Patients with TMB-low tumors were associated with significantly shorter PFS and OS durations than those with TMB-high tumors: [median PFS, 2.3 months (95% CI, 0.9–not reached) vs. 15.6 months (95% CI, 4.4–not reached); HR, 6.20 (95% CI, 1.93–19.98), $P = 0.002$] and [median OS, 6.5 months (95% CI, 1.5–not reached) vs. 25.7 months (95% CI, 8.4–not reached); HR, 3.77 (95% CI, 1.25–11.30), $P < 0.001$; **Fig. 3A** and **B**]. Multivariate analyses showed that a low TMB was independently associated with short PFS [HR, 4.72 (95% CI, 1.41–15.75), $P = 0.012$; Supplementary Table S2] and OS [HR, 3.39 (95% CI, 1.11–10.30), $P = 0.032$; Supplementary Table S3). After excluding patients with pembrolizumab plus napabucasin, a low TMB was still a significant predictor of a negative response [median PFS, 2.3 months (95% CI, 0.9–not reached) vs. 9.6 months (95% CI, 4.4–not reached); HR, 5.41 (95% CI, 1.65–17.78), $P = 0.005$ and median OS, 6.5 months (95% CI, 1.5–not reached) vs. 25.7 months (95% CI, 6.0–not reached); HR, 3.19 (95% CI, 1.05–9.74), $P = 0.031$].

In contrast, patients with *FGFR2, TCF7, NOTCH1*, or *POLE* mutations tended to have a higher ORR than those with without mutations in these genes (**Table 2**). Among the patients, those with tumors with either *NOTCH1* or *POLE* mutations had a significantly higher TMB than tumors without these mutations [median TMB: *NOTCH1*, 46.1 muts/Mb (range, 8.5–93.0) vs. 29.5 muts/Mb (range, 3.6–59.7), $P = 0.004$; *POLE*, 50.6 muts/Mb (range, 20.3–83.6) vs. 37.5 muts/Mb (range, 3.6–93.0), $P = 0.021$, respectively]. No significant difference in the ORR was observed according to PD-L1 expression (46.2% with PD-L1 CPS < 1 vs. 33.3% with 1 ≤ CPS < 10 vs. 46.2% with CPS ≥ 10, respectively, $P = 0.916$; **Table 2**).

Published OnlineFirst April 29, 2021; DOI: 10.1158/1078-0432.CCR-21-0401

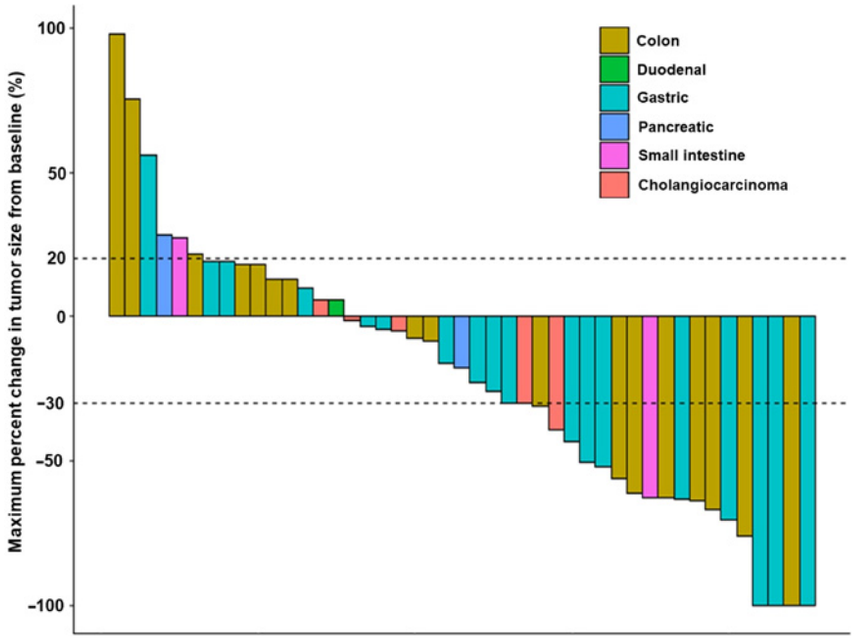

Figure 1.
Waterfall plot of the maximum percentage change in tumor size from baseline as measured using the RECIST version 1.1. All patients had measurable lesions. In the overall population, the ORR and DCR were 44.4% (20 of 45 patients) and 84.4% (38 of 45 patients), respectively.

We next examined whether particular gene mutations or expression patterns were associated with response to PD-1 blockade. Among 34 common gene alterations in GI tumors, only patients with mutant *PTEN* ($n = 14$) showed a significant correlation with a lower ORR than those with wild-type *PTEN* [$n = 31$; 21.4% vs. 54.8%; odds: 4.45 (95% CI, 1.03–19.20), $P = 0.045$; **Table 2**]. Patients with mutant *PTEN* had a significantly higher TMB than those with wild-type *PTEN* [median TMB (range); 43.2 (29.9–93.0) muts/Mb vs. 20.3 (3.6–83.6) muts/Mb, $P = 0.017$]. *PTEN* mutations and a TMB-low status were mutually exclusive. Patients with mutant *PTEN* tended to experience shorter PFS and OS durations than those with wild-type *PTEN* [median PFS, 4.3 months (95% CI, 1.2–not reached) vs. 15.6 months (95% CI, 4.3–not reached); HR, 1.72 (95% CI, 0.76–3.92), $P = 0.195$] and [median OS, 15.2 months (95% CI, 3.8–not reached) vs. 25.7 months (95% CI, 10.3–not reached); HR, 1.46 (95% CI, 0.62–3.46), $P = 0.391$], although the difference was not statistically significant (Supplementary Fig. S2A and S2B).

Next, we further divided the mutation sites of *PTEN* into the phosphatase and C2 domains in accordance with a previous report (18), and patients with *PTEN* mutations in the phosphatase domain [$n = 8$; ORR: 12.5% vs. 54.8%, $P = 0.049$; median PFS, 2.6 months (95% CI, 0.6–4.4) vs. 15.6 months (95% CI, 4.3–not reached); HR, 5.04 (95% CI, 2.00–12.68), $P < 0.001$] exhibited a significantly lower ORR and experienced a shorter PFS and OS than those with wild-type *PTEN* [$n = 31$; median OS, 6.0 months (95% CI, 1.1–15.2) vs. 25.7 months (95% CI, 10.3–not reached); HR, 2.81 (95% CI, 1.13–6.96], $P = 0.026$; **Fig. 3C** and **D**]. In contrast, there was no significant difference between the patients with *PTEN* mutations in the C2 domain [$n = 6$; ORR: 33.3% vs. 54.8%, $P = 0.405$; median PFS, not reached (95% CI, 1.2–not reached) vs. 15.6 months (95% CI, 4.3–not reached); HR, 0.55 (95% CI, 0.20–1.51), $P = 0.243$] and those with wild-type *PTEN* [$n = 31$; median OS, not reached (95% CI, 3.8–not reached) vs. 25.7 months (95% CI, 10.3–not reached); HR, 0.58 (95% CI, 0.21–1.59), $P = 0.288$; **Fig. 3C** and **D**]. Patient characteristics according to the *PTEN* mutational status are summarized in Supplementary Table S4. Multivariate analyses showed that *PTEN* mutations in the phosphatase domain were independently associated with a shorter PFS [HR, 12.61 (95% CI, 3.75–42.35), $P < 0.001$; Supplementary Table S5] and OS [HR, 8.92 (95% CI, 2.60–30.55), $P < 0.001$; Supplementary Table S6]. After excluding patients with pembrolizumab plus napabucasin, *PTEN* mutations in the phosphatase domain was still a significant predictor of a negative response [median PFS, 1.7 months (95% CI, 0.6–4.2) vs. 9.6 months (95% CI, 4.0–not reached); HR, 5.11 (95% CI, 1.90–13.70), $P = 0.001$; median OS, 6.0 months (95% CI, 1.1–not reached) vs. 16.1 months (95% CI, 7.3–not reached); HR, 2.61 (95% CI, 0.98–6.98), $P = 0.055$]. Also, after excluding TMB-low tumors, *PTEN* mutation in the phosphatase domain was still a significant predictor of a negative response [median PFS, 2.6 months (95% CI, 0.6–4.4) vs. not reached (95% CI, 7.4–not reached); HR, 7.86 (95% CI, 2.79–22.10], $P < 0.001$; median OS, 6.0 months (95% CI, 1.1–15.2) vs. not reached (95% CI, 11.1–not reached); HR, 3.47 (95% CI, 1.33–9.07), $P = 0.011$]. Importantly, among the 20 patients showing disease progression within 6 months after the initiation of PD-1 blockade, four had TMB-low tumors (20%), and eight (40%) had *PTEN* mutations in the phosphatase domain.

Tumor microenvironment according to the *PTEN* mutational status

We next examined whether the *PTEN* mutation status was associated with levels of immune infiltrate in patient tumors. Representative CT of patients with wild-type *PTEN* (best response, PR) and those with *PTEN* mutations in the phosphatase domain (best response, PD) obtained during the treatment is shown in **Fig. 4A** and **B**, and representative multiplex IHC images before the treatment are shown in **Fig. 4C**. Analysis of the tumor microenvironment by multiplex fluorescence IHC revealed that tumors with *PTEN* phosphatase domain mutations had significantly lower levels of intratumoral $CD8^+$ T cells and higher levels of intratumoral $CD204^+$ macrophages than tumors with wild-type *PTEN*, resulting in a higher intratumoral $CD204^+$ macrophage/$CD3^+$ T-cell ratio [median levels of carcinoma $CD8^+$ T cells, 127.9/mm^2 (IQR, 64.6–131.7) vs. 336.0/mm^2 (IQR, 177.6–686.5), $P = 0.019$; median levels of intratumoral $CD204^+$

Published OnlineFirst April 29, 2021; DOI: 10.1158/1078-0432.CCR-21-0401

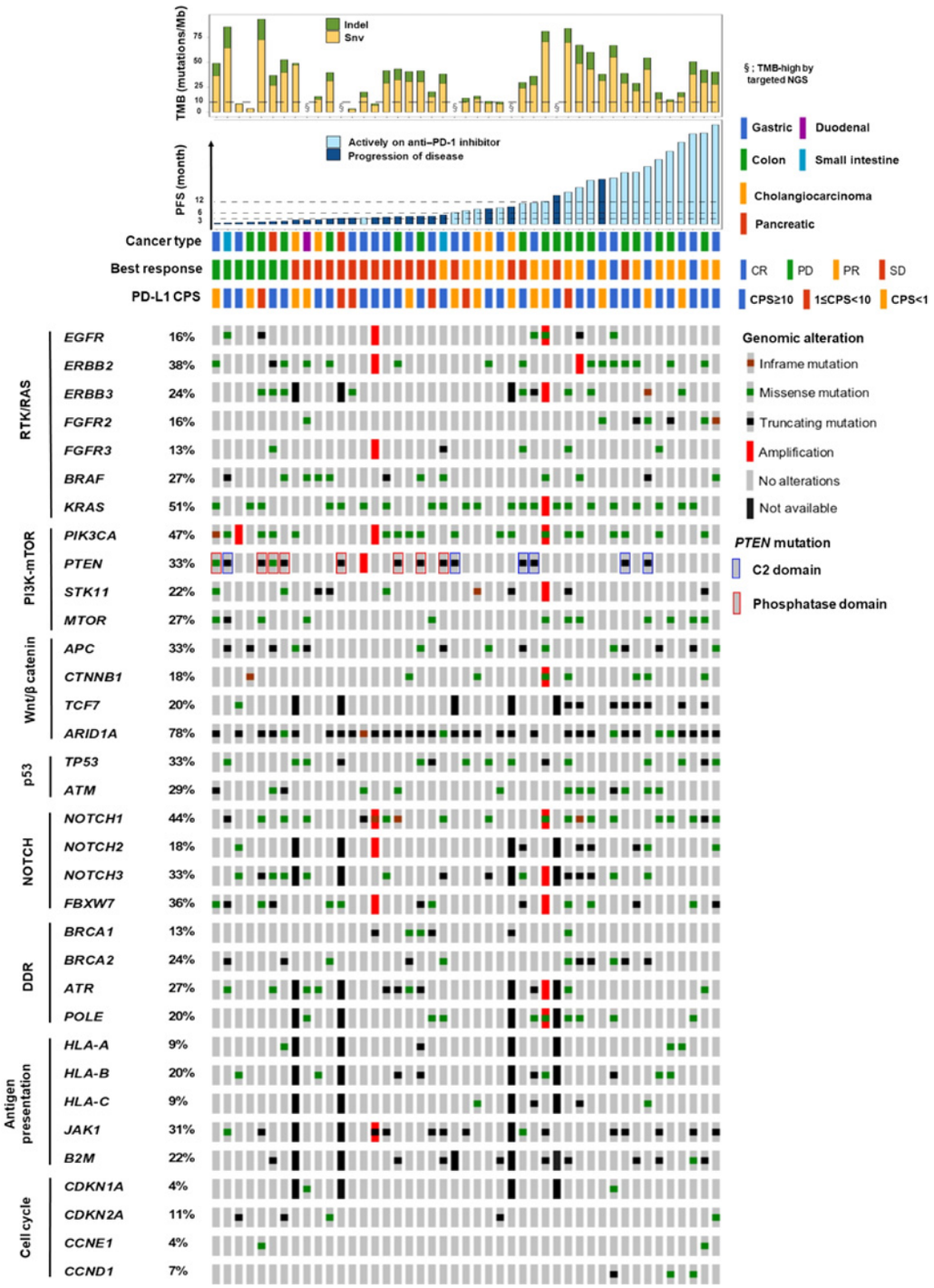

Figure 2.

Comprehensive molecular characterization of MSI-H or dMMR GI tumors with PD-1 blockade. WES-assessed TMB values of each patient were shown at the top (yellow: snv, green: indel). Distributions and annotations of individual gene alterations in the study cohort as assessed by WES- or NGS-targeted gene panel analysis are shown. Each column represents one patient. Abbreviations: PD, progressive disease.

macrophages: 732.6/mm^2 (IQR, 609.9–1037.5) vs. 421.3/mm^2 (IQR, 237.8–587.8), $P = 0.037$; and median ratio of intratumoral CD204$^+$ macrophages/CD3$^+$ T cells, 5.9 (IQR, 3.5–6.7) vs. 1.8 (IQR, 0.54–3.74), $P = 0.045$; **Fig. 4C**]. On the other hand, there was no statistically significant difference in these components between tumors with *PTEN* C2 mutations and those with wild-type *PTEN* [median levels of intratumoral CD8$^+$ T cells, 206.7/mm^2 (IQR, 75.8–256.9) vs. 336.0/mm^2 (IQR, 177.6–686.5), $P = 0.120$; median levels of

Published OnlineFirst April 29, 2021; DOI: 10.1158/1078-0432.CCR-21-0401

Table 2. Objective tumor responses according to TMB, gene mutations, and the PD-L1 CPS.

		Detected	(%)	Responder (CR or PR)	Nonresponder (SD or PD)	ORR (%)	OR	95% CI		P^a
TMB	High	41	(91.1)	20	21	(48.8)				
	Low	4	(8.9)	0	4	(0.0)				
EGFR	Wild-type	40	(88.9)	17	23	(42.5)	(Reference)			0.464
	Mutant	5	(11.1)	3	2	(60.0)	0.49	0.07	3.28	
ERBB2	Wild-type	29	(64.4)	13	16	(44.8)	(Reference)			0.944
	Mutant	16	(35.6)	7	9	(43.8)	1.04	0.31	3.57	
ERBB3	Wild-type	32	(76.2)	14	18	(43.8)	(Reference)			0.373
	Mutant	10	(23.8)	6	4	(60.0)	0.52	0.12	2.20	
FGFR2	Wild-type	38	(84.4)	14	24	(36.8)	(Reference)			0.039
	Mutant	7	(15.6)	6	1	(85.7)	0.1	0.01	0.89	
FGFR3	Wild-type	40	(88.9)	17	23	(42.5)	(Reference)			0.464
	Mutant	5	(11.1)	3	2	(60.0)	0.49	0.07	3.28	
BRAF	Wild-type	33	(73.3)	15	18	(45.5)	(Reference)			0.821
	Mutant	12	(26.7)	5	7	(41.7)	1.17	0.31	4.44	
KRAS	Wild-type	23	(51.1)	9	14	(39.1)	(Reference)			0.464
	Mutant	22	(48.9)	11	11	(50.0)	0.64	0.20	2.10	
PIK3CA	Wild-type	25	(55.6)	13	12	(52.0)	(Reference)			0.257
	Mutant	20	(44.4)	7	13	(35.0)	2.01	0.60	6.74	
PTEN	Wild-type	31	(68.9)	17	14	(54.8)	(Reference)			0.045
	Mutant	14	(31.1)	3	11	(21.4)	4.45	1.03	19.20	
STK11	Wild-type	36	(80.0)	17	19	(47.2)	(Reference)			0.457
	Mutant	9	(20.0)	3	6	(33.3)	1.79	0.39	8.29	
MTOR	Wild-type	33	(73.3)	13	20	(39.4)	(Reference)			0.263
	Mutant	12	(26.7)	7	5	(58.3)	0.46	0.12	1.78	
APC	Wild-type	30	(66.7)	13	17	(43.3)	(Reference)			0.832
	Mutant	15	(33.3)	7	8	(46.7)	0.87	0.25	3.04	
CTNNB1	Wild-type	37	(82.2)	14	23	(37.8)	(Reference)			0.071
	Mutant	8	(17.8)	6	2	(75.0)	0.2	0.04	1.15	
TCF7	Wild-type	32	(78.0)	13	19	(40.6)	(Reference)			0.063
	Mutant	9	(22.0)	7	2	(77.8)	0.2	0.03	1.09	
ARID1A	Wild-type	11	(24.4)	4	7	(36.4)	(Reference)			0.536
	Mutant	34	(75.6)	16	18	(47.1)	0.64	0.16	2.61	
TP53	Wild-type	30	(66.7)	11	19	(36.7)	(Reference)			0.142
	Mutant	15	(33.3)	9	6	(60.0)	0.39	0.11	1.38	
ATM	Wild-type	29	(70.7)	14	15	(48.3)	(Reference)			0.920
	Mutant	12	(29.3)	6	6	(50.0)	0.93	0.24	3.58	
NOTCH1	Wild-type	25	(55.6)	8	17	(32.0)	(Reference)			0.064
	Mutant	20	(44.4)	12	8	(60.0)	0.31	0.09	1.07	
NOTCH2	Wild-type	34	(82.9)	15	19	(44.1)	(Reference)			0.203
	Mutant	7	(17.1)	5	2	(71.4)	0.32	0.05	1.86	
NOTCH3	Wild-type	27	(65.9)	13	14	(48.1)	(Reference)			0.910
	Mutant	14	(34.1)	7	7	(50.0)	0.93	0.26	3.38	
FBXW7	Wild-type	31	(68.9	15	16	(48.4)	(Reference)			0.430
	Mutant	14	(31.1)	5	9	(35.7)	1.69	0.46	6.20	
BRCA1	Wild-type	39	(86.7)	19	20	(48.7)	(Reference)			0.172
	Mutant	6	(13.3)	1	5	(16.7)	4.75	0.51	44.50	
BRCA2	Wild-type	33	(73.3)	14	19	(42.4)	(Reference)			0.652
	Mutant	12	(26.7)	6	6	(50.0)	0.74	0.20	2.77	
ATR	Wild-type	30	(73.2)	17	13	(56.7)	(Reference)			0.105
	Mutant	11	(26.8)	3	8	(27.3)	3.49	0.77	15.80	
POLE	Wild-type	32	(78.0)	13	19	(40.6)	(Reference)			0.063
	Mutant	9	(22.0)	7	2	(77.8)	0.2	0.03	1.09	
HLA-A	Wild-type	36	(90.0)	17	19	(47.2)	(Reference)			0.916
	Mutant	4	(10.0)	2	2	(50.0)	0.9	0.11	7.06	
HLA-B	Wild-type	32	(80.0)	15	17	(46.9)	(Reference)			0.874
	Mutant	8	(20.0)	4	4	(50.0)	0.88	0.19	4.16	
HLA-C	Wild-type	37	(92.5)	16	21	(43.2)	(Reference)			
	Mutant	3	(7.5)	3	0	(100.0)	Not available			
JAK1	Wild-type	28	(66.7)	13	15	(46.4)	(Reference)			0.827
	Mutant	14	(33.3)	7	7	(50.0)	0.87	0.24	3.13	
B2M	Wild-type	31	(77.5)	13	18	(41.9)	(Reference)			0.073
	Mutant	9	(22.5)	7	2	(77.8)	0.21	0.04	1.16	

(Continued on the following page)

Published OnlineFirst April 29, 2021; DOI: 10.1158/1078-0432.CCR-21-0401

Table 2. Objective tumor responses according to TMB, gene mutations, and the PD-L1 CPS. (Cont'd)

		Detected	(%)	Responder (CR or PR)	Nonresponder (SD or PD)	ORR (%)	OR	95% CI		P^a
CDKN1A	Wild-type	39	(95.1)	19	20	(48.7)	(Reference)			0.972
	Mutant	2	(4.9)	1	1	(50.0)	0.95	0.06	16.30	
CDKN2A	Wild-type	39	(86.7)	17	22	(43.6)	(Reference)			0.769
	Mutant	6	(13.3)	3	3	(50.0)	0.77	0.14	4.32	
CCNE1	Wild-type	43	(95.6)	19	24	(44.2)	(Reference)			0.872
	Mutant	2	(4.4)	1	1	(50.0)	0.79	0.05	13.50	
CCND1	Wild-type	42	(93.3)	17	25	(40.5)	(Reference)			
	Mutant	3	(6.7)	3	0	(100.0)	Not available			
PD-L1 CPS	CPS < 1	13	(28.9)	6	7	(46.2)	(Reference)			
	1 ≤ CPS < 10	6	(13.3)	2	4	(33.3)	1.71	0.23	12.90	0.601
	CPS ≥ 10	26	(57.8)	12	14	(46.2)	1	0.26	3.80	1.000

Abbreviations: ECOG, Eastern Cooperative Oncology Group; PS, Performance status; PD, progressive disease; PD-L1, programmed death ligand 1.
[a]*P* values were calculated using the logistic regression method.

intratumoral $CD204^+$ macrophages: 620.0/mm^2 (IQR, 476.6–765.3) vs. 421.3/mm^2 (IQR, 237.8–587.8), $P = 0.223$; and median ratio of intratumoral $CD204^+$ macrophages/$CD3^+$ T cells, 1.8 (IQR, 0.9 to 2.8) vs. 1.11 (IQR, 0.54–3.74), $P = 0.946$; **Fig. 4C**). IHC analysis showed that the PTEN-positive tumor area was significantly smaller in tumors with *PTEN* phosphatase domain mutations than in those with wild-type *PTEN* (Supplementary Fig. S3A). In summary, *PTEN* mutations in phosphatase domain had an immunosuppressive microenvironment characterized by increased infiltration of tumor-associated macrophages and may affect PTEN protein expression.

The activation of PI3K/AKT/mTOR pathway according to the *PTEN* mutational status

Because *PTEN* is an important suppressor of the PI3K/AKT/mTOR pathway, transcriptome analysis was performed to investigate the impact of *PTEN* mutation status on the signaling pathway. In transcriptomic analysis, compared with that in tumors with wild-type *PTEN*, the expression of *PTEN* mRNA was significantly lower in tumors with *PTEN* mutations in the phosphatase domain but not in those with mutations in the C2 domain (Supplementary Fig. S3B). GSEA demonstrated an enrichment of genes involved in the PI3K–AKT–mTOR (Supplementary Fig. S4A) and MTORC1 (Supplementary Fig. S4B) signaling pathways in tumors with *PTEN* phosphatase domain mutations compared with those with wild-type *PTEN*, whereas the difference was not statistically significant between tumors with mutant *PTEN*/mutations in the C2 domain and those with wild-type *PTEN* (Supplementary Fig. S4C and S4D).

Discussion

We genomically profiled patients with MSI-H/dMMR GI tumors receiving PD-1 blockade to elucidate the predictors of response to immune checkpoint inhibitors. The majority of samples were evaluated by WES, and the others were evaluated with NGS. In addition, we evaluated the tumor microenvironment by transcriptomic analysis and multiplex fluorescence IHC. To the best of our knowledge, this is the first report to provide a comprehensive description of the molecular landscape of tumors with various responses to PD-1 blockade in patients with MSI-H/dMMR GI cancer.

In our cohort, TMB-low tumors were associated with poorer clinical outcomes following anti–PD-1 therapies than TMB-high tumors, in line with a previous report on MSI-H/dMMR colorectal cancer (12). Recently, the phase II KEYNOTE-158 study showed that TMB-high solid tumors treated with pembrolizumab were associated with a higher ORR [30.3% (27.1% in MSS) vs. 6.7%] than TMB-low tumors, leading to the FDA approval of pembrolizumab for the treatment of TMB-high solid tumors (19). The findings from the KEYNOTE-158 study suggest that TMB might be a useful biomarker of immune checkpoint inhibitors in MSS/pMMR tumors. Also, our study showed that TMB might be a predictive biomarker of these agents in MSI-H/dMMR tumors. However, optimal cutoff value, as well as the impact of TMB on the efficacy of these agents, warrants further investigation in larger cohorts. Moreover, previous reports demonstrated almost all MSI-H tumors show a high mutation load regardless of primary cancer sites (20, 21), whereas some reports about patients with various cancer types demonstrated that a few MSI-H patients did not show TMB-H (22, 23). Reports about the association between MSI-H and TMB-H in patients with GI tumors are limited, and further examinations are needed.

In our study, among mutations in genes in common oncogenic signaling pathways, only *PTEN* mutations were significantly correlated with a low ORR after PD-1 blockade in a mutually exclusive manner with TMB-low tumors. This observation is consistent with previous reports demonstrating an enrichment of *PTEN* mutations in PD-1 nonresponders with MSS/pMMR glioblastoma or uterine leiomyosarcoma (24, 25). Notably, in our study, *PTEN* mutations in the phosphatase domain were associated with a significantly lower ORR and shorter PFS and OS than wild-type *PTEN*, whereas *PTEN* mutations in the C2 domain were not. Moreover, immunosuppressive tumor microenvironments with significantly fewer $CD8^+$ T cells and increased tumor-associated macrophages were observed in tumors with *PTEN* mutations in the phosphatase domain. These findings are in accordance with those of previous studies showing that *PTEN*-mutated tumors or the loss of PTEN tended to increase macrophage infiltration or decrease $CD8^+$ T-cell infiltration in glioblastoma and melanoma (24, 26). In addition, tumors with *PTEN* mutations in the phosphatase domain were significantly associated with low levels of *PTEN* mRNA expression and loss of the PTEN protein, resulting in enrichment of the PI3K/AKT/mTOR and MTORC1 signaling pathways. These findings suggest that *PTEN* mutations in the phosphatase domain are correlated with PTEN loss of function, leading to resistance to PD-1 blockade. The response to anti–PD-1/PD-1 therapies according to the location of the *PTEN* mutations warrants further evaluation in future studies.

Published OnlineFirst April 29, 2021; DOI: 10.1158/1078-0432.CCR-21-0401

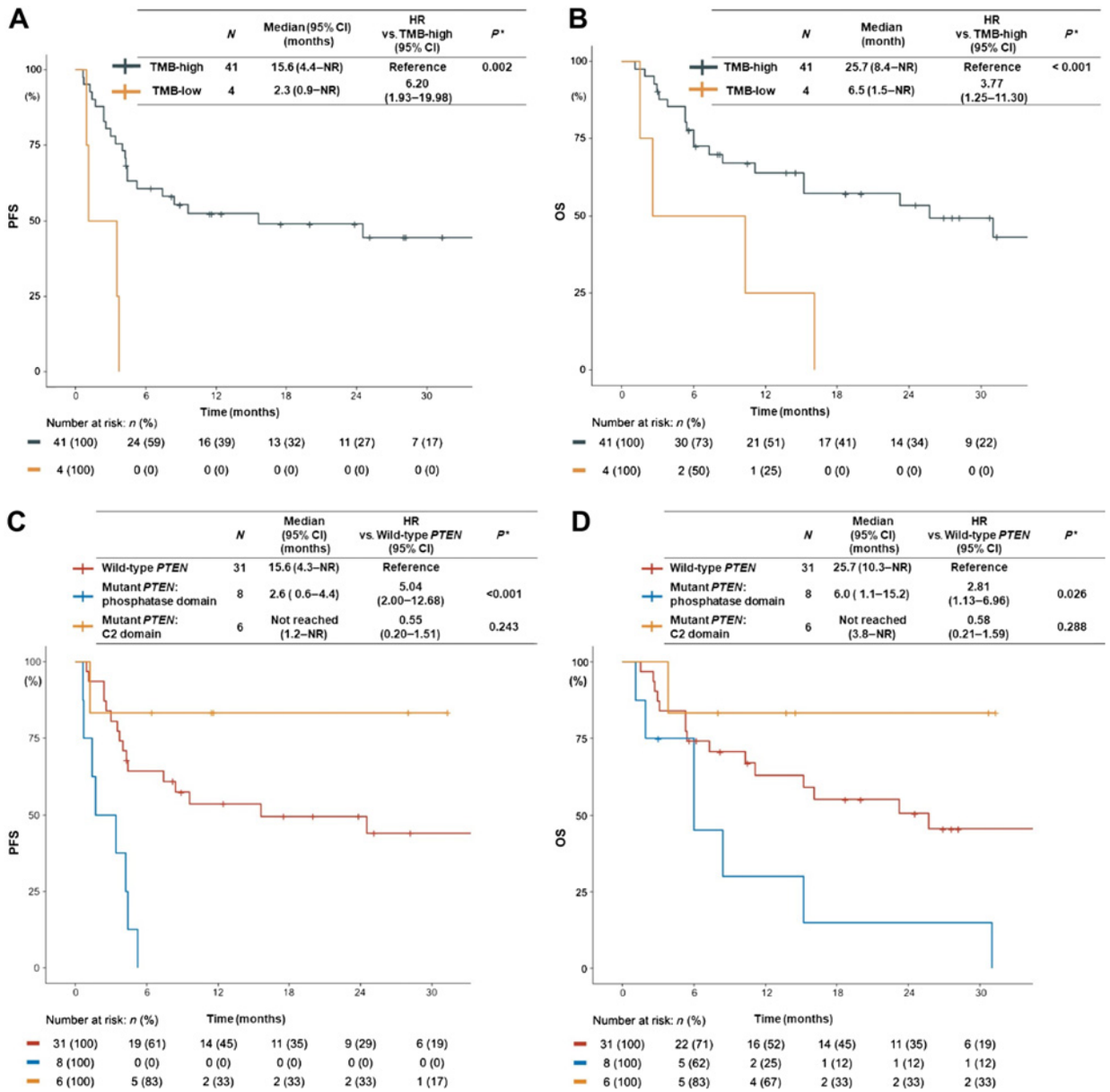

Figure 3.

A, Kaplan–Meier plots of PFS according to TMB. **B,** OS according to TMB. Patients with TMB-low showed significantly lower PFS and OS than those with TMB-high: [median PFS, 2.3 months (95% CI, 0.9–not reached) vs. 15.6 months (95% CI, 4.4–not reached); HR, 6.20 (95% CI, 1.93–19.98), $P = 0.002$] and [median OS, 6.5 months (95% CI, 1.5–not reached) vs. 25.7 months (95% CI, 8.4–not reached); HR, 3.77 (95% CI, 1.25–11.30), $P < 0.001$]. *P values were calculated using the Cox proportional hazards model. **C,** Kaplan–Meier plots of PFS according to the *PTEN* mutation domain. Patients with *PTEN* mutations in the phosphatase domain experienced a shorter PFS and OS than those with wild-type *PTEN* [median PFS, 2.6 months (95% CI, 0.6–4.4) vs. 15.6 months (95% CI, 4.3–not reached); HR, 5.04 (95% CI, 2.00–12.68), $P < 0.001$]. In contrast, there was no significant difference between the patients with *PTEN* mutations in the C2 domain and those with wild-type PTEN [median PFS, not reached (95% CI, 1.2–not reached) vs. 15.6 months (95% CI, 4.3–not reached); HR, 0.55 (95% CI, 0.20–1.51), $P = 0.243$]. *P values were calculated using the Cox proportional hazards model. **D,** OS according to the PTEN mutation domain. Patients with *PTEN* mutations in the phosphatase domain experienced a shorter OS than those with wild-type *PTEN* [median OS, 6.0 months (95% CI, 1.1–15.2) vs. 25.7 months (95% CI, 10.3–not reached); HR, 2.81 (95% CI, 1.13–6.96), $P = 0.026$]. In contrast, there was no significant difference between the patients with *PTEN* mutations in the C2 domain and those with wild-type [median OS, not reached (95% CI, 3.8–not reached) vs. 25.7 months (95% CI, 10.3–not reached); HR, 0.58 (95% CI, 0.21–1.59), $P = 0.288$]. *P values were calculated using the Cox proportional hazards model.

Importantly, among the 20 patients showing disease progression within 6 months after PD-1 blockade, four had TMB-low tumors (20%), and eight (40%) had *PTEN* mutations in the phosphatase domain. Other gene alterations, such as *STK11, FBXW7, JAK1, B2M*, and *HLA* mutations, which have been reported to be associated with resistance to immune checkpoint inhibitors (10, 27–29), were also observed in nonresponders, although tumors with these mutations were not associated with a significantly low ORR in our study. The

Published OnlineFirst April 29, 2021; DOI: 10.1158/1078-0432.CCR-21-0401

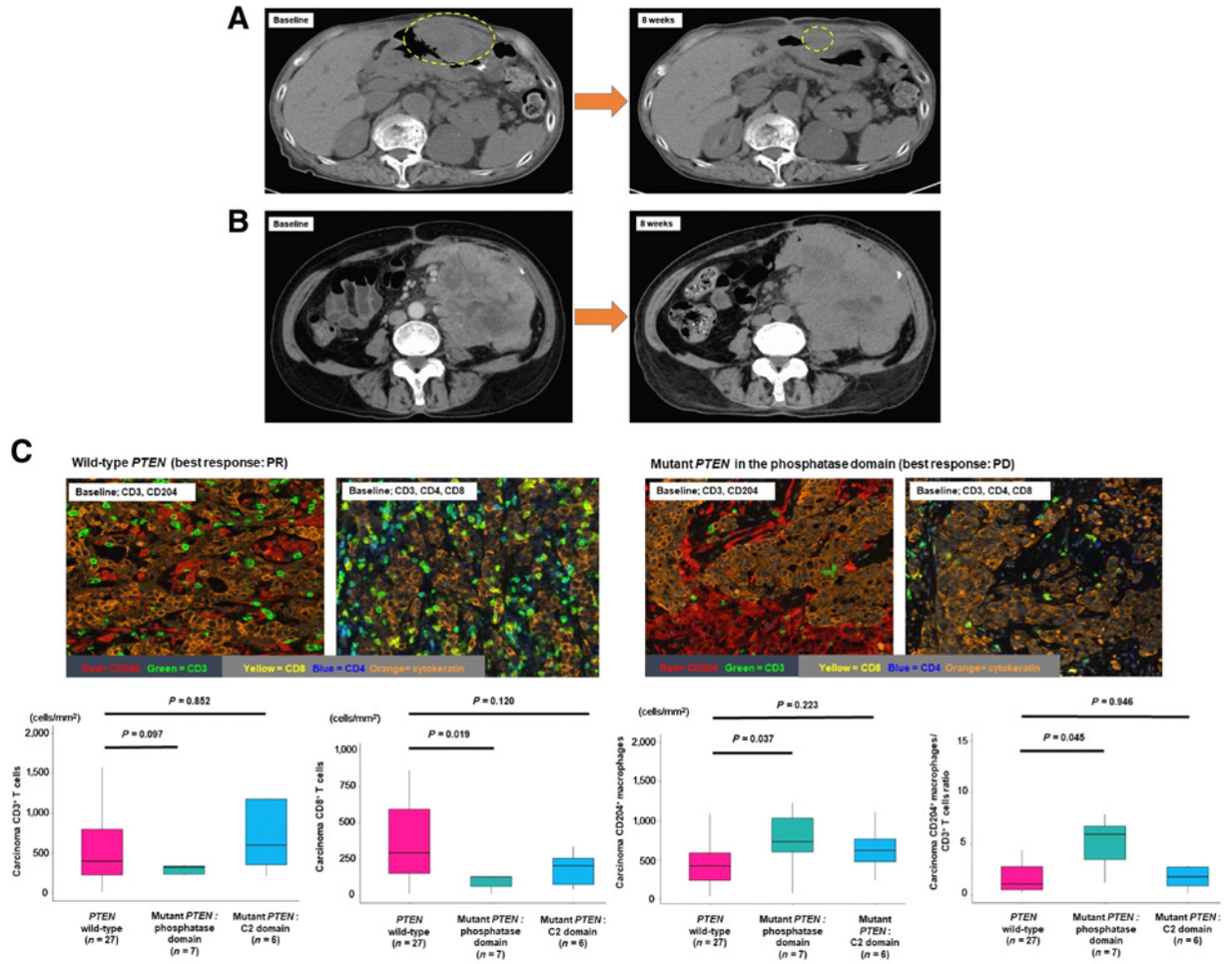

Figure 4.

CT during treatment in patients with wild-type *PTEN* (best response, PR, **A**) and mutant *PTEN* in the phosphatase domain (best response, PD, **B**). Representative CT with wild-type *PTEN* (best response, PR) and those with *PTEN* mutations in the phosphatase domain (best response, PD) during the treatment are shown. **C,** Multiplex fluorescence IHC analysis according to *PTEN* mutations. Representative multiplex IHC images of patients with wild-*PTEN* (best response, PR) and those with *PTEN* mutations in the phosphatase domain (best response, PD) before the treatment are shown. The yellow dotted line indicates lymph node metastasis. CD204, CD3, CD8, CD4, and cytokeratin in cells are shown in red, green, yellow, blue, and orange, respectively. Tumors with *PTEN* phosphatase domain mutations had significantly lower levels of intratumoral $CD8^+$ T cells and higher levels of intratumoral $CD204^+$ macrophages than tumors with wild-type *PTEN*, resulting in a higher intratumoral $CD204^+$ macrophage/$CD3^+$ T-cell ratio. On the other hand, there was no statistically significant difference in these components between tumors with *PTEN* C2 mutations and those with wild-type *PTEN.*

levels of intratumoral $CD3^+$, $CD8^+$ T cells, and $CD204^+$ macrophages were not different according to *JAK1* or *B2M* mutational status (data not shown). The impact of these mutations on efficacies of immune checkpoint inhibitors and tumor microenvironment warrants further investigations. In contrast, tumors with *NOTCH1, POLE, FGFR2*, or *TCF7* mutations in our study tended to be associated with a higher ORR than those without mutations in these genes. In addition, MSI-H/dMMR GI tumors with *NOTCH1* or *POLE* mutations were associated with a significantly higher TMB than wild-type tumors. Our findings in MSI-H/dMMR GI tumors were in line with those from previous reports demonstrating that MSS/pMMR tumors with *NOTCH* or *POLE* mutations had a higher TMB than those without these mutations, resulting in favorable clinical outcomes after treatment with immune checkpoint inhibitors (11, 30, 31). The precise mechanism regarding the association of these mutations with a high ORR in our study on the efficacy of PD-1/PD-L1 blockade should be investigated in the near future.

The major limitations of this study were its small sample size and retrospective, single-center design. Also, this study might be complicated by the heterogeneity of the patient population including the different primary tumor sites, though the FDA approved pembrolizumab for MSI-H/dMMR solid tumors regardless of tumor histology. Moreover, we included the patients with pembrolizumab plus napabucasin, leading to the heterogeneous population in this study. However, given that MSI-H/dMMR is a rare subtype in patients with GI tumors (32), our study provides new insight into the development of predictive biomarkers or combination therapies for PD-1/PD-L1 blockade in this population.

In conclusion, TMB-low tumors and *PTEN* mutations, especially in the phosphatase domain with immunosuppressive microenvironments, might be associated with less responsiveness to PD-1 blockade in a mutually exclusive manner in MSI-H/dMMR GI tumors, which warrants further investigation in larger cohorts. Considering that *PTEN* mutations are frequently observed in MSI-H/dMMR tumors (33, 34), the mutational status of *PTEN* could be an important predictive biomarker in this population receiving anti–PD-1/PD-L1 therapies. Moreover, targeting immunesuppressive cells using tyrosine kinase inhibitors such as VEGF inhibitors might overcome resistance to immune checkpoint inhibitors in MSI-H/dMMR tumors with *PTEN* mutations harboring abundant tumor-associated macrophages (35, 36).

Authors' Disclosures

A. Kawazoe reports grants from MSD, Ono, and Sumitomo Dainippon outside the submitted work. Y. Nakamura reports grants from Guardant Health, Genomedia, Taiho Pharmaceutical, and Chugai Pharmaceutical outside the submitted work. T. Kuwata reports grants from Government (Japan), Daiichi-Sankyo, and Ono Pharmaceutical, and personal fees from MSD, AstraZeneca, and Taiho Pharma outside the submitted work. Y. Kuboki reports grants and personal fees from Taiho and Ono; personal fees from Bayer, Sanofi, and Eli Lilly; and grants from Takeda, AstraZeneca, Daiichi-Sankyo, Boehringer Ingelheim, Amgen, Chugai, and GSK outside the submitted work. D. Kotani reports personal fees from Takeda, Chugai, Eli Lilly, Merck Biopharma, Taiho, Ono, and Bristol Myers Squibb outside the submitted work. T. Kojima reports grants and personal fees from Ono Pharmaceutical and MSD; grants from Astellas Amgen BioPharma, Taiho Pharmaceutical, Chugai Pharmaceutical, and Shionogi; and personal fees from Oncolys BioPharma, Astellas Pharma, BMS, and Merck outside the submitted work. H. Taniguchi reports grants from Sysmex, Roche Diagnostics KK, and Daiichi-Sankyo; grants and personal fees from Taiho and Takeda; and personal fees from Eli Lilly, Chugai, and Merck Biopharma outside the submitted work. H. Mano reports grants from Ono Pharmaceutical, Daiichi Sankyo, PFDeNA, and Konica Minolta; and personal fees from Chugai and CureGene outside the submitted work. M. Ikeda reports grants and personal fees from AstraZeneca, ASLAN, Bayer, Bristol Myers Squibb, Chugai, EA Pharma, Eli Lilly, Eisai, MSD, Nihon Servier, Novartis, Takeda, and Yakult; personal fees from Astellas, Gilead, Otsuka, Sumitomo Dainippon, Taiho, and Teijin Pharma; and grants from Chiome Bioscience, GlaxoSmithKline, J-Pharma, Merck Serono, Ono, and Pfizer outside the submitted work. K. Shitara reports grants and personal fees from Astellas Pharma, Ono Pharmaceutical, Taiho Pharmaceutical, and Merck Pharmaceutical; grants from Eli Lilly and Company, Dainippon Sumitomo Pharma, Daiichi Sankyo, Chugai Pharma, Medi Science, and Eisai; and personal fees from Bristol Myers Squibb, Takeda Pharmaceuticals, Pfizer Inc., Novartis, AbbVie Inc., Yakult, GlaxoSmithKline, Amgen, and Boehringer Ingelheim outside the submitted work. I. Endo reports grants from Taiho Pharmaceutical, Yakult Honsha, Chugai Pharmaceutical, and Ono Pharmaceutical outside the submitted work. T. Yoshino reports grants and personal fees from Chugai; personal fees from Takeda, Eli Lilly, and Merck Biopharma; and grants from GlaxoSmithKline, Novartis, Sanofi, Ono, Daiichi-Sankyo, Parexel, and Sumitomo Dainippon outside the submitted work. No disclosures were reported by the other authors.

Authors' Contributions

K. Chida: Conceptualization, data curation, formal analysis, investigation, visualization, writing–original draft, writing–review and editing. **A. Kawazoe:** Conceptualization, supervision, investigation, writing–original draft, writing–review and editing. **M. Kawazu:** Conceptualization, formal analysis, supervision, investigation, writing–review and editing. **T. Suzuki:** Conceptualization, formal analysis, supervision, validation, methodology, writing–review and editing. **Y. Nakamura:** Supervision, writing–review and editing. **T. Nakatsura:** Writing–review and editing. **T. Kuwata:** Investigation, writing–review and editing. **T. Ueno:** Formal analysis, writing–review and editing. **Y. Kuboki:** Writing–review and editing. **D. Kotani:** Supervision, writing–review and editing. **T. Kojima:** Writing–review and editing. **H. Taniguchi:** Writing–review and editing. **H. Mano:** Writing–review and editing. **M. Ikeda:** Supervision, writing–review and editing. **K. Shitara:** Supervision, writing–review and editing. **I. Endo:** Writing–review and editing. **T. Yoshino:** Conceptualization, supervision, writing–review and editing.

Acknowledgments

The authors would like to thank all patients and families for participating and M. Takahashi and K. Takenouchi for their assistance with multiplex fluorescence IHC. They would also like to thank Nature Research Editing Service (https://authorservices.springernature.com) for the English language review.

This study was supported by research funding from the National Cancer Center Hospital East and the Japan Agency for Medical Research and Development (AMED; JP19cm0106502 to M. Kawazu).

The costs of publication of this article were defrayed in part by the payment of page charges. This article must therefore be hereby marked *advertisement* in accordance with 18 U.S.C. Section 1734 solely to indicate this fact.

Received February 1, 2021; revised March 9, 2021; accepted April 27, 2021; published first April 29, 2021.

References

1. Xiao Y, Freeman GJ. The microsatellite instable subset of colorectal cancer is a particularly good candidate for checkpoint blockade immunotherapy. Cancer Discov 2015;5:16–18.
2. Li K, Luo H, Huang L, Luo H, Zhu X. Microsatellite instability: a review of what the oncologist should know. Cancer Cell Int 2020;20:16.
3. Marabelle A, Le DT, Ascierto PA, Di Giacomo AM, De Jesus-Acosta A, Delord J-P, et al. Efficacy of Pembrolizumab in patients with noncolorectal high microsatellite instability/mismatch repair–deficient cancer: results from the phase II KEYNOTE-158 study. J Clin Oncol 2020; 38:1–10.
4. Le DT, Kim TW, Van Cutsem E, Geva R, Jäger D, Hara H, et al. Phase II open-label study of pembrolizumab in treatment-refractory, microsatellite instability-high/mismatch repair-deficient metastatic colorectal cancer: KEYNOTE-164. J Clin Oncol Official J Am Soc Clin Oncol 2019;38: 11–19.
5. André T, Shiu K-K, Kim TW, Jensen BV, Jensen LH, Punt C, et al. Pembrolizumab in microsatellite-instability-high advanced colorectal cancer. New Engl J Medicine 2020;383:2207–18.
6. Fuchs CS, Doi T, Jang RW, Muro K, Satoh T, Machado M, et al. Safety and efficacy of pembrolizumab monotherapy in patients with previously treated advanced gastric and gastroesophageal junction cancer: phase 2 clinical KEYNOTE-059 trial. Jama Oncol 2018;4:e180013.
7. Shitara K, Özgüroğlu M, Bang Y-J, Di Bartolomeo M, Mandalà M, Ryu M-H, et al. Pembrolizumab versus paclitaxel for previously treated, advanced gastric or gastro-oesophageal junction cancer (KEYNOTE-061): a randomised, open-label, controlled, phase 3 trial. Lancet 2018;392:123–33.
8. Patel SP, Kurzrock R. PD-L1 expression as a predictive biomarker in cancer immunotherapy. Mol Cancer Ther 2015;14:847–56.
9. Barroso-Sousa R, Keenan TE, Pernas S, Exman P, Jain E, Garrido-Castro AC, et al. Tumor mutational burden and PTEN alterations as molecular correlates of response to PD-1/L1 blockade in metastatic triple-negative breast cancer. Clin Cancer Res 2020;26:2565–72.
10. Zaretsky JM, Garcia-Diaz A, Shin DS, Escuin-Ordinas H, Hugo W, Hu-Lieskovan S, et al. Mutations associated with acquired resistance to PD-1 blockade in melanoma. New Engl J Medicine 2016;375:819–29.
11. Zhang K, Hong X, Song Z, Xu Y, Li C, Wang G, et al. Identification of deleterious NOTCH mutation as novel predictor to efficacious immunotherapy in NSCLC. Clin Cancer Res 2020;26:3649–61.
12. Schrock AB, Ouyang C, Sandhu J, Sokol E, Jin D, Ross JS, et al. Tumor mutational burden is predictive of response to immune checkpoint inhibitors in MSI-high metastatic colorectal cancer. Ann Oncol 2019;30:1096–103.
13. Kawazoe A, Kuboki Y, Shinozaki E, Hara H, Nishina T, Komatsu Y, et al. Multicenter phase I/II trial of napabucasin and pembrolizumab in patients with metastatic colorectal cancer (EPOC1503/SCOOP Trial). Clin Cancer Res 2020; 26:5887–94.
14. Bacher JW, Flanagan LA, Smalley RL, Nassif NA, Burgart LJ, Halberg RB, et al. Development of a fluorescent multiplex assay for detection of MSI-high tumors. Dis Markers 2004;20:237–50.

15. Sanchez-Vega F, Mina M, Armenia J, Chatila WK, Luna A, La KC, et al. Oncogenic signaling pathways in The Cancer Genome Atlas. Cell 2018;173:321–37.
16. Nakamura Y, Taniguchi H, Ikeda M, Bando H, Kato K, Morizane C, et al. Clinical utility of circulating tumor DNA sequencing in advanced gastrointestinal cancer: SCRUM-Japan GI-SCREEN and GOZILA studies. Nat Med 2020;26:1859–64.
17. Subramanian A, Tamayo P, Mootha VK, Mukherjee S, Ebert BL, Gillette MA, et al. Gene set enrichment analysis: A knowledge-based approach for interpreting genome-wide expression profiles. P Natl Acad Sci Usa 2005;102:15545–50.
18. Yehia L, Ngeow J, Eng C. PTEN-opathies: from biological insights to evidence-based precision medicine. J Clin Invest 2019;129:452–64.
19. Marabelle A, Fakih M, Lopez J, Shah M, Shapira-Frommer R, Nakagawa K, et al. Association of tumour mutational burden with outcomes in patients with advanced solid tumours treated with pembrolizumab: prospective biomarker analysis of the multicohort, open-label, phase 2 KEYNOTE-158 study. Lancet Oncol 2020;21:1353–65.
20. Chalmers ZR, Connelly CF, Fabrizio D, Gay L, Ali SM, Ennis R, et al. Analysis of 100,000 human cancer genomes reveals the landscape of tumor mutational burden. Genome Med 2017;9:34.
21. Network T. Comprehensive molecular characterization of gastric adenocarcinoma. Nature 2014;513:202.
22. Vanderwalde A, Spetzler D, Xiao N, Gatalica Z, Marshall J. Microsatellite instability status determined by next-generation sequencing and compared with PD-L1 and tumor mutational burden in 11,348 patients. Cancer Med 2018;7:746–56.
23. Wyrwicz LS, Lee K-W, Cutsem EV, Bang Y-J, Fuchs CS, Kudaba I, et al. Association of TMB using the foundation medicine companion diagnostic (F1CDx) with efficacy of first-line pembrolizumab (pembro) or pembro plus chemotherapy (pembro + chemo) versus chemo in patients with gastric cancer (gc) from KEYNOTE-062. Ann Oncol 2020;31:S907–8.
24. Zhao J, Chen AX, Gartrell RD, Silverman AM, Aparicio L, Chu T, et al. Immune and genomic correlates of response to anti-PD-1 immunotherapy in glioblastoma. Nat Med 2019;25:462–9.
25. George S, Miao D, Demetri GD, Adeegbe D, Rodig SJ, Shukla S, et al. Loss of PTEN Is associated with resistance to anti-PD-1 checkpoint blockade therapy in metastatic uterine leiomyosarcoma. Immunity 2017;46:197–204.
26. Peng W, Chen JQ, Liu C, Malu S, Creasy C, Tetzlaff MT, et al. Loss of PTEN promotes resistance to T cell–mediated immunotherapy. Cancer Discov 2016;6:202–16.
27. Wang H, Guo J, Shang X, Wang Z. Less immune cell infiltration and worse prognosis after immunotherapy for patients with lung adenocarcinoma who harbored STK11 mutation. Int Immunopharmacol 2020;84:106574.
28. Gstalder C, Liu D, Miao D, Lutterbach B, DeVine AL, Lin C, et al. Inactivation of Fbxw7 impairs dsRNA sensing and confers resistance to PD-1 blockade. 2020;10:1296–311.
29. Montesion M, Murugesan K, Jin DX, Sharaf R, Sanchez N, Guria A, et al. Somatic HLA class I loss is a widespread mechanism of immune evasion which refines the use of tumor mutational burden as a biomarker of checkpoint inhibitor response. Cancer Discov 2020;11:282–92.
30. Jiang D, Niu Z, Zhang J, Wang Y, Shang L, Li B, et al. Notch family gene mutations associate with high tumor mutational burden in diverse cancers. J Clin Oncol 2019;37:e14616–.
31. Yao J, Gong Y, Zhao W, Han Z, Guo S, Liu H, et al. Comprehensive analysis of POLE and POLD1 Gene Variations identifies cancer patients potentially benefit from immunotherapy in Chinese population. Sci Rep-uk 2019;9:15767.
32. Le DT, Durham JN, Smith KN, Wang H, Bartlett BR, Aulakh LK, et al. Mismatch repair deficiency predicts response of solid tumors to PD-1 blockade. Science 2017;357:409–13.
33. Kim B, Kang SY, Kim D, Heo YJ, Kim K-M. PTEN protein loss and loss-of-function mutations in gastric cancers: the relationship with microsatellite instability, EBV, HER2, and PD-L1 expression. Cancers 2020;12:1724.
34. Zhou X-P, Loukola A, Salovaara R, Nystrom-Lahti M, Peltomäki P, de la Chapelle A, et al. PTEN mutational spectra, expression levels, and subcellular localization in microsatellite stable and unstable colorectal cancers. Am J Pathology 2002;161:439–47.
35. Kato Y, Tabata K, Kimura T, Yachie-Kinoshita A, Ozawa Y, Yamada K, et al. Lenvatinib plus anti-PD-1 antibody combination treatment activates CD8+ T cells through reduction of tumor-associated macrophage and activation of the interferon pathway. PLoS One 2019;14:e0212513.
36. Kawazoe A, Fukuoka S, Nakamura Y, Kuboki Y, Wakabayashi M, Nomura S, et al. Lenvatinib plus pembrolizumab in patients with advanced gastric cancer in the first-line or second-line setting (EPOC1706): an open-label, single-arm, phase 2 trial. Lancet Oncol 2020;21:1057–65.

Published OnlineFirst April 29, 2021; DOI: 10.1158/1078-0432.CCR-21-0401

Clinical Cancer Research

A Low Tumor Mutational Burden and *PTEN* Mutations Are Predictors of a Negative Response to PD-1 Blockade in MSI-H/dMMR Gastrointestinal Tumors

Keigo Chida, Akihito Kawazoe, Masahito Kawazu, et al.

Clin Cancer Res 2021;27:3714-3724. Published OnlineFirst April 29, 2021.

論文目録

I. 主論文

A Low Tumor Mutational Burden and *PTEN* Mutations Are Predictors of a Negative Response to PD-1 Blockade in MSI-H/dMMR Gastrointestinal Tumors

Chida K, Kawazoe A, Kawazu M, Suzuki T, Nakamura Y, Nakatsura T, Kuwata T, Ueno T, Kuboki Y, Kotani D, Kojima T, Taniguchi H, Mano H, Ikeda M, Shitara K, Endo I, Yoshino T.

Journal: Clinical Cancer Research. 2021;27(13):3714-3724

II. 副論文

1. Diagnosis and Treatment of HER2-Positive Metastatic Colorectal Cancer.
   Chida K, Nakamura Y.
   Gan To Kagaku Ryoho. 2020;47(11):1565-1569.
2. Survival Benefit of Crossover Administration of Regorafenib and Trifluridine/Tipiracil Hydrochloride for Patients With Metastatic Colorectal Cancer: Exploratory Analysis of a Japanese Society for Cancer of the Colon and Rectum Multicenter Observational Study (REGOTAS).
   Chida K, Kotani D, Moriwaki T, Fukuoka S, Masuishi T, Takashima A, Kumekawa Y, Kajiwara T, Yamazaki K, Komoda M, Makiyama A, Denda T, Hatachi Y, Suto T, Sugimoto N, Enomoto M, Ishikawa T, Kashiwada T, Ando K, Yuki S, Okita Y, Kusaba H, Sakai D, Okamoto K, Tamura T, Yamashita K, Gosho M, Shimada Y.
   Front Oncol. 2021;11:576036.
3. Efficacy and safety of trifluridine/tipiracil plus bevacizumab and trifluridine/tipiracil or regorafenib monotherapy for chemorefractory metastatic colorectal cancer: a retrospective study
   Chida K, Kotani D, Nakamura Y, Kawazoe A, Kuboki Y, Shitara K, Kojima T, Taniguchi H, Watanabe J, Endo I, Yoshino T.
   Ther Adv Med Oncol. 20210;13:17588359211009143.
4. The Prognostic Impact of *KRAS* G12C Mutation in Patients with Metastatic Colorectal Cancer: A Multicenter Retrospective Observational Study
   Chida K, Kotani D, Masuishi T, Kawakami T, Kawamoto Y, Kato K, Fushiki K, Sawada K, Kumanishi R, Shirasu H, Matsubara Y, Yuki S, Komatsu Y, Yamazaki K, Yoshino T.
   Oncologist. 2021. doi: 10.1002/onco.13870. Online ahead of print.